PCCP

Accepted Manuscript

Volume 1 | Number 1 | Jan 2013 | Pages 1–100

PCCP

Physical Chemistry Chemical Physics

www.rsc.org/pccp

ROYAL SOCIETY OF CHEMISTRY

ROYAL SOCIETY OF CHEMISTRY

www.rsc.org/pccp

Ternary $B_2X_2H_2$ (X = O and S) rhombic clusters and their potential use as inorganic ligands in sandwich-type $(B_2X_2H_2)_2Ni$ complexes

Da-Zhi Li,*[a] Li-Juan Zhang,[a] Ting Ou,[b] Hai-Xia Zhang,[a] Ling Pei,[a]
Hua-Jin Zhai*[bc] and Si-Dian Li*[b]

---

[a] *Binzhou Key Laboratory of Materials Chemistry, Department of Chemical Engineering, Binzhou University, Binzhou 256603, P. R. China.*
E-mail: ldz005@126.com, dazhili@bzu.edu.cn (D.Z.L.)

[b] *Nanocluster Laboratory, Institute of Molecular Science, Shanxi University, Taiyuan 030006, P. R. China.*
E-mail: hj.zhai@sxu.edu.cn (H.J.Z.); lisidian@sxu.edu.cn (S.D.L.)

[c] *State Key Laboratory of Quantum Optics and Quantum Optics Devices, Shanxi University, Taiyuan 030006, P. R. China*

Abstract

Based upon global searches and electronic structure calculations at the B3LYP and CCSD(T) levels, we present the global-minimum structures of two ternary B-O-H and B-S-H rhombic clusters: D_{2h} $B_2O_2H_2$ (**1**, ^1A_g) and C_{2v} $B_2S_2H_2$ (**2**, $^1A_1$). Both species feature a B_2X_2 (X = O or S) four-membered ring as the core, with two H atoms attached terminally. The former cluster is perfectly planar, whereas the latter undergoes a slight butterfly distortion. Bonding analyses reveal a four-center four-electron (4c-4e) o-bond in these clusters, which are 4π systems in the *nonbonding*/*bonding* combination, in contrast to the *antibonding*/*bonding* combination in a classical 4π antiaromatic hydrocarbon such as cyclobutadiene (C_4H_4). The **1** and **2** clusters are considered to be aromatic. The present results also help elucidate the bonding nature in the relevant heteroatomic ring $B_2N_2H_4$ system and suggest that it is not appropriate to consider $B_2N_2H_4$ as an inorganic cyclobutadiene, a conception that has been in existence in the literature for over 40 years. The electronic properties of the global-minimum **1** and **2** clusters are predicted. It is shown that $B_2O_2H_2$ (**1**) and $B_2S_2H_2$ (**2**) may serve as effective inorganic ligands to form sandwich-type transition metal complexes, such as D_{2d} $[B_2O_2H_2]_2Ni$ (**3**) and D_{2d} $[B_2S_2H_2]_2Ni$ (**4**).

Introduction

As a prototypical electron-deficient element in the periodic table, boron has rich chemistry. Elemental boron clusters[1–6] and boron-containing compound clusters[7–14] show intriguing structural and bonding properties. Notably, boron clusters possess unique planar or quasi-planar structures in a wide range of sizes (up to at least 40 atoms),[4] which are aromatic or antiaromatic following the Hückel rules and show close analogy to the organic hydrocarbon molecules. Oxidation of boron clusters results in boron oxide clusters and boron boronyl (BO) clusters,[8] which are anticipated to be even more electron-deficient. Nonetheless, the binary B-O and isovalent B-S clusters can make use of the O 2p or S 3p lone-pairs for exotic chemical bonds.

In the B-O and B-S clusters, the heteroatomic BX (X = O, S) rings appear to be critical structural blocks, facilitating the formation of ternary molecular species and beyond, via the attachment of terminal ligands. Among these ternary B-X-H molecules are the boroxine ($B_3O_3H_3$) and borazine ($B_3N_3H_6$),[14–21] which possess a hexagonal B_3X_3 (X = O or N) ring as the core and are considered as inorganic analogues of benzene. A boron oxide analogue of boroxine, B_6O_6, was recently discovered computationally.[9] Named as the boronyl boroxine, B_6O_6 can be alternatively formulated as $B_3O_3(BO)_3$, in which three BO groups substitute the three H terminals in $B_3O_3H_3$. Since both BO and H are monovalent σ radicals, B_6O_6 and $B_3O_3H_3$ are isovalent with each other, rendering B_6O_6 another inorganic analogue of benzene. Similar to benzene, D_{3h} $B_3O_3X_3$ (X = BO, H) can be used as ligands to form transition metal complexes, such as the sandwich-type D_{3d} $(B_3O_3X_3)_2Cr$,[9] D_{3d} $(B_3O_3X_3)_2V$,[10] and the perfectly planar $(B_3O_3H_3)_nM^+$ (n = 1, 2; M = Cu, Ag, Au) complexes.[11]

Boron-containing compound clusters can also possess the rhombic B_2X_2 structural core. However, our current understanding of the structural principles and bonding nature of such species remains inadequate. A few previously reported examples include $B_2N_2H_4$,[22,23] which was proposed in the 1970s to be the boron-nitrogen hydride analogue of cyclobutadiene (C_4H_4). Consequently, $B_2N_2H_4$ has long been considered as an antiaromatic species with 4π electrons, according to the 4*n* Hückel rule for antiaromaticity, similar to cyclobutadiene. However, a recent report concluded that $B_2N_2H_4$ and its isovalent $N_2P_2F_4$ species are aromatic,[24] on the basis of the nucleus-independent chemical shift (NICS) calculations. The bonding nature of $B_2N_2H_4$ has thus been a long-standing issue of debate, for which we would like to offer an in-depth understanding through the current study on the title clusters.

Recently, the four-membered B_2O_2 rhombic ring is also characterized in boron oxide clusters.[25] Similar, isovalent B_2S_2 ring should be present in boron sulfide clusters. Here we explore the ternary B-X-H (X = O or S) clusters, $B_2X_2H_2$ to be more specific, on the basis of the B_2X_2 core via the attachment of terminal H ligands. The work involves global-minimum searches, electronic structure calculations at the density-functional theory (DFT) and coupled-cluster theory (CCSD(T)) levels, and chemical bonding and aromaticity analyses. The global minima of D_{2h} $B_2O_2H_2$ (**1**) and C_{2v} $B_2S_2H_2$ (**2**) exhibit perfectly planar and slightly distorted structures, respectively, with the four-membered B_2X_2 heteroatomic rings. Canonical molecular orbital (CMO) analysis and adaptive natural density partitioning (AdNDP)[26] reveal that $B_2O_2H_2$ (**1**) and $B_2S_2H_2$ (**2**) are 4π systems with a *nonbonding*/*bonding* combination for the two π CMOs. Such a 4π system has been proposed recently to be a rhombic four-center four-electron (4c-4e) π bond, or the o-bond.[25] This bonding pattern differs markedly from that in cyclobutadiene; the latter features an *antibonding*/*bonding* combination for the two CMOs, resulting in antiaromaticity and a rectangular structural distortion. In the four-membered ring systems, aromaticity follows the order of $B_2S_2H_2$ (**2**) > $B_2N_2H_4$ > $B_2O_2H_2$ (**1**) > C_4H_4 (antiaromatic). The larger electronegativity difference between B and X (X = N, O, and S), the weaker aromaticity for the system. To assess the viability of D_{2h} $B_2O_2H_2$ (**1**) and C_{2v} $B_2S_2H_2$ (**2**) as potential ligands for coordination compounds, we explore the viability of their sandwich-type transition metal complexes: D_{2d} $[B_2O_2H_2]_2Ni$ (**3**) and D_{2d} $[B_2S_2H_2]_2Ni$ (**4**), the latter being particularly promising with a substantial formation energy. In these complexes, the $B_2O_2H_2$ (**1**) or $B_2S_2H_2$ (**2**) clusters are stabilized by a Ni atom and their structural and chemical integrity is well maintained.

Computational Details

The global-minimum searches for $B_2X_2H_2$ (X = O and S) were conducted using the Gradient Embedded Genetic Algorithm (GEGA)[27,28] and Coalescence Kick (CK)[29,30] programs. Subsequent full structural optimizations and frequency calculations were carried out for the low-lying isomers using the hybrid B3LYP method[31,32] with the basis set of aug-cc-pVTZ, as implemented in the Gaussian 03 package.[33] For the sandwich complexes, the Stuttgart relativistic small core basis set and effective core potential (Stuttgart RSC 1997 ECP)[34] was employed for Ni. We performed full optimization for these complexes by taking into consideration of different spin-multiplicity states. Furthermore, the relative energies were refined for the low-lying isomers of $B_2X_2H_2$ (X=O and S) using the single-point CCSD(T) calculations[35–37] at the B3LYP geometries. AdNDP,[26] in combination with the CMO analysis, was used to elucidate the chemical bonding. The NBO 5.0 program[38] was used to calculate the natural atomic charges.

Results and Discussion

Perfectly planar D_{2h} $B_2O_2H_2$ with a rhombic B_2O_2 ring

The global-minimum structure of $B_2O_2H_2$ is illustrated in Fig. 1, along with that of $B_2S_2H_2$. Alternative optimized low-lying structures of $B_2O_2H_2$ are shown in Fig. 2. The global-minimum $B_2O_2H_2$ (**1**, ^1A_g) is perfectly planar with D_{2h} symmetry, which lies 0.46 and 0.67 eV lower than the second low-lying isomer, C_s $B_2O_2H_2$, at the B3LYP and single-point CCSD(T) levels, respectively. The calculated B-O distance for the rhombic B_2O_2 ring (1.40 Å) in **1** should be roughly viewed as, or slightly stronger than single bonds, which is comparable to those in the B_2O_2 cores of the C_{2v} B_3O_3 and C_s B_3O_4 clusters.[25] The $B_2O_2H_2$ (**1**) cluster may be constructed by connecting two terminal H to a B_2O_2 core, analogous to the situation of boroxine, D_{3h} $B_3O_3H_3$.[15–17] The latter species can be viewed as three H terminals attaching to a B_3O_3 ring. It is speculated that by combining terminal H with the B_2O_2 or B_3O_3 rings in certain energetically favorable ways, one may be able to establish a general structural pattern for the B-O-H ternary system, which is worthy of pursuit in the future.

D_{2h} $B_2O_2H_2$ (**1**, ^1A_g) is a simple cluster. Its bonding can be understood via the AdNDP analysis. As an extension of natural bond orbital (NBO) analysis, AdNDP[26] represents the electronic structure of a molecular system in terms of *n*-center two-electron (*n*c-2e) bonds, where the values of *n* range from one to the total number of atoms in the system. AdNDP thus recovers not only the classical Lewis bonding elements (lone pair and 2c-2e bonds), but also the delocalized *n*c-2e bonds. As presented in Fig. 3, $B_2O_2H_2$ (**1**) possesses 20 valence electrons, among which 4 are for the two 1c-2e O 2p lone-pairs, 8 are for four 2c-2e B-O single bonds within the B_2O_2 ring, and 4 are responsible for two 2c-2e B-H single bonds, which are the classical Lewis elements. The remaining 4 electrons are responsible for the global bonding in the B_2O_2 ring, including a delocalized 4c-4e π bond, as well as a 2c-2e π “bond”.

The global bonding elements are also obvious in the CMOs, as shown in Fig. 4 (top panel). Here the highest occupied molecular orbital (HOMO) is a 2c-2e π “bond” and the HOMO−4 is a completely delocalized 4c-4e π bond. The former is a formally antibonding combination of the O 2p atomic orbitals (AOs). However, due to the large distance between the two O atoms (~2.1 Å), the overlap of the O 2p AOs in the HOMO is negligible and the “antibonding” interaction is practically zero, and it is thus more appropriate to classify this HOMO as a nonbonding orbital, which contributes very little (if any) to the stability of the species. In short, HOMO−4 and HOMO form a unique bonding/nonbonding π combination, in contrast to the bonding/antibonding combination for a typical four-membered ring antiaromatic π system. A similar bonding pattern was described recently in the boron oxide clusters and a concept of the rhombic 4c-4e bond, that is, the o-bond, was proposed.[25] The global-minimum D_{2h} $B_2O_2H_2$ (**1**, ^1A_g) cluster is a new example for the o-bond.

Comparison of the ternary B-O-H and B-S-H clusters: D_{2h} $B_2O_2H_2$ *versus* C_{2v} $B_2S_2H_2$

Given the similarity between S and O in their electron configurations, a closely similar structure of $B_2S_2H_2$ (**2**, C_{2v}, $^1A_1$) (Fig. 1) is obtained upon structural searches and subsequent

B3LYP/aug-cc-pVTZ optimization. $B_2S_2H_2$ (**2**) can be constructed by attaching two H terminals to a rhombic B_2S_2 ring. Indeed, this turns out to be the global-minimum structure of the $B_2S_2H_2$ system (Fig. 5). A D_{2h} structure is very close in energy within less than 0.05 eV, but it is a transition state with an imaginary frequency of 108.14*i* cm^{-1} at the B3LYP level. The $B_2S_2H_2$ (**2**, C_{2v}, $^1A_1$) global minimum is also reasonably well-defined, being at least 0.40 and 0.54 eV lower than alternative structure at the B3LYP and single-point CCSD(T) levels, respectively.

Different from D_{2h} $B_2O_2H_2$ (**1**, ^1A_g), there exists a slight nonplanar, butterfly distortion in $B_2S_2H_2$ (**2**, C_{2v}, $^1A_1$), which can be seen more clearly from the side view (Fig. 1). This slightly puckered structure has a dihedral angle of 161.9°. The nonplanarity is attributed to the more pronounced contraction of the s orbitals as compared to the corresponding p orbitals in the heavier element S, and therefore its hybridization with p orbitals becomes more difficult. In other words, in the case of S, the three-fold coordination does not show pronounced s contribution in its hybridization, such as in sp^2, but instead it prefers a triangular pyramidal configuration. Similar slightly distorted structures have also been found previously in other four-membered heterocyclic compounds.[24,39] In $B_2S_2H_2$ (**2**, C_{2v}, $^1A_1$), the B-S distance within the B_2S_2 ring is 1.83 Å, which is close to a B-S single bond.

In terms of chemical bonding, the AdNDP analysis (Fig. 6) suggests that $B_2S_2H_2$ (**2**, C_{2v}, $^1A_1$) share the same overall bonding pattern relative to $B_2O_2H_2$ (**1**, D_{2h}, ^1A_g). In particular, $B_2S_2H_2$ (**2**, C_{2v}, $^1A_1$) also features a rhombic 4c-4e π bond (that is, the o-bond), whose bonding/nonbonding π combination (HOMO−3/HOMO) is compared with that of $B_2O_2H_2$ (**1**, D_{2h}, ^1A_g) in Fig. 4. The natural atomic charges from the NBO analysis in **2** are $q_B = 0.16$ |e| and $q_S = -0.11$ |e| (Table 1), suggesting that the B-S interaction is remarkably covalent. This is in contrast to the B-O bonding in **1**, which is highly polar: $q_B = 0.95$ |e| and $q_S = -0.86$ |e|.

Four-membered ring systems with 4π electrons: Rhombic D_{2h} $B_2O_2H_2$ and C_{2v} $B_2S_2H_2$ versus rectangular cyclobutadiene

Both the D_{2h} $B_2O_2H_2$ (**1**, ^1A_g) and C_{2v} $B_2S_2H_2$ (**2**, $^1A_1$) global-minimum clusters possess a heteroatomic four-membered B_2X_2 (X = O and S) ring as the core, with two terminal H groups attached. The core is of rhombus-type, with a slight butterfly distortion in **2**. Notably, the four B-X distances in the B_2X_2 ring are equivalent (Fig. 1), in contrast to the rectangular distortion in the cyclobutadiene. Cyclobutadiene is a prototypical antiaromatic species with 4π electrons, following the 4*n* Hückel rule for antiaromaticity.

There has been quite a long history for computational studies on the relevant heteroatomic inorganic systems, dated back as early as the 1970s. Among these is D_{2h} $B_2N_2H_4$,[22,24] in which each B and N atom is terminated by one H. The early proposal suggested that D_{2h} $B_2N_2H_4$ is an inorganic analogue of cyclobutadiene,[22] which are indeed isovalent species. However, a recent computational study concluded that D_{2h} $B_2N_2H_4$ is aromatic rather than antiaromatic, with a negative NICS of −2.921 ppm. For comparison, cyclobutadiene has a highly positive NICS value of 35.763 ppm.[24] We revisited the $B_2N_2H_4$ cluster here. However, different to the reported results of Baird,[22] D_{2h} $B_2N_2H_4$ turns out to be a transition state with an imaginary frequency of 201.79*i* cm^{-1} at the B3LYP/aug-cc-pVTZ level. The global minimum of $B_2N_2H_4$ is a slightly distorted C_{2v} structure, similar to $B_2S_2H_2$ (**2**, $^1A_1$). This structure is in consistent with that of Pati and coworkers.[24]

The D_{2h} $B_2O_2H_2$ (**1**, ^1A_g) and C_{2v} $B_2S_2H_2$ (**2**, $^1A_1$) clusters provide an opportunity to resolve the above paradox in the chemical bonding of heteroatomic four-membered systems. We believe the key lies in the nature of the upper π CMO, that is, the HOMO (Fig. 4): It is essentially nonbonding in **1** or **2**, whereas it is strongly antibonding in cyclobutadiene. The latter results in significant electronic destabilization in cyclobutadiene and underlies its square-to-rectangular structural distortion, which are characteristic of a 4π antiaromatic system. In the D_{2h} $B_2O_2H_2$ (**1**) and C_{2v} $B_2S_2H_2$ (**2**) clusters, the nonbonding HOMO (b_{1g}) and HOMO (b_1), respectively, contribute very little in term of electronic stabilization/destabilization of the systems. Thus, although they each possess 4π electrons, the **1** and **2** clusters feature a rhombic 4c-4e o-bond and can be practically considered as 2π systems. Only the completely bonding 2π electrons, that is, HOMO−4 (b_{3u}) and HOMO−1 (a_1), respectively, govern the structures and electronic stability of the clusters; and only these 2π electrons count in the Hückel rule. Indeed, our calculated $NICS_{zz}(0)$ for **1**, **2**, and cyclobutadiene are −1.21, −6.11, and 17.76 ppm, respectively. The corresponding $NICS_{zz}(1)$ are 3.85, −0.76, and 55.96 ppm, respectively. These NICS values indicate that **1** and **2** are remarkably different from cyclobutadiene in terms of aromaticity/antiaromaticity. It is suitable to classify the **1** and **2** species as aromatic.

When one considers a NH group to be equivalent to O (that is, a N-H bond to be equal to an O lone-pair), the D_{2h} or C_{2v} $B_2N_2H_4$ species[22,24] becomes isovalent to **1** and **2**. The D_{2h} and C_{2v} $B_2N_2H_4$ species also possess 4π electrons,[22,24] in the nonbonding/bonding combination, and thus $B_2N_2H_4$ is also an aromatic system. It appears not to be appropriate to view $B_2N_2H_4$ as an inorganic analogue of cyclobutadiene, despite the 40-year long history of the conception.[22] Our calculations show that C_{2v} $B_2N_2H_4$ has the $NICS_{zz}(0)$ and $NICS_{zz}(1)$ values of −2.98 and 0.21 ppm, respectively, which are also very different from those of cyclobutadiene. In the four-membered ring systems, the aromaticity roughly follows the order of $B_2S_2H_2$ (**2**) > C_{2v} $B_2N_2H_4$ > $B_2O_2H_2$ (**1**) > C_4H_4 (antiaromatic). In the former three species with o-bonds, the larger electronegativity difference between B and X (X = N, O, and S), the weaker aromaticity for the heteroatomic system. This is understandable because in a system with a smaller electronegativity difference between B and X, the B-X bond is less polar and the π electrons can be more delocalized in the ring; and vice versa.

It is important to note that the 4c-4e o-bond in **1**, **2**, and $B_2N_2H_4$ manages to make use of two O/N 2p lone pairs to form a delocalized, completely bonding 4c-2e π bond along with a "residual" nonbonding orbital. This delocalization potency of the O/N 2p AOs in the boron related systems helps compensate for boron's intrinsic electron-deficiency.

Predicted electronic properties for D_{2h} $B_2O_2H_2$ and C_{2v} $B_2S_2H_2$

To aid future experimental characterizations of D_{2h} $B_2O_2H_2$ (**1**, ^1A_g) and C_{2v} $B_2S_2H_2$ (**2**, $^1A_1$), we report their calculated electronic properties. The vertical ionization potentials (VIPs) are predicted at the B3LYP/aug-cc-pVTZ level to be 12.25 and 9.55 eV for **1** and **2**, respectively

(Table 1), whereas the calculated HOMO–LUMO energy gaps are 4.02 and 5.29 eV, respectively. Thus, **1** and **2** are relatively stable species.

The infrared (IR) spectra of D_{2h} $B_2O_2H_2$ (**1**, ^1A_g) and C_{2v} $B_2S_2H_2$ (**2**, $^1A_1$) have been simulated at the B3LYP/aug-cc-pVTZ level, as shown in Fig. 7. The IR spectra are rather similar with each other for the two species, except for a spectral shift. Note that there is an intense peak in **1** at 2724 cm^{-1}, which corresponds to the B-H symmetric stretching mode. Another intense peak at 1344 cm^{-1} corresponds to the B-O symmetric stretching. For **2**, the B-H stretching mode is at 2683 cm^{-1}, whereas the B-S stretching is located at 774 cm^{-1}. Comparison of the B-H symmetric stretchings in **1** and **2** reveals a red shift in **2**, hinting for the stronger B-H interaction in **1**.

D_{2h} $B_2O_2H_2$ and C_{2v} $B_2S_2H_2$ as potential ligands in the sandwich-type complexes

Boroxine ($B_3O_3H_3$) and boronyl boroxine (D_{3h} B_6O_6) have been explored for thermally stable, magnetic compounds.[9–11] Similarly, the $B_2N_2H_4$ cluster as ligands to form full-sandwich transition metal complexes has been studied.[40] Sandwich $(C_2P_2R_2)_2Ni$ complex with staggered D_{2d} symmetry has been synthesized by Wettling and coworkers, in which $C_2P_2R_2$ with a C_2P_2 ring is used as a ligand.[41] Here, attempt to pursue the sandwich-type transition metal complexes by using the D_{2h} $B_2O_2H_2$ (**1**) and C_{2v} $B_2S_2H_2$ (**2**) clusters as ligands, which feature the 4c-4e o-bond. Figure 8 shows the optimized structures of D_{2d} $(B_2O_2H_2)_2Ni$ (**3**) and D_{2d} $(B_2S_2H_2)_2Ni$ (**4**) sandwich complexes at the B3LYP level, which are compared with that based on the cyclobutadiene, D_{4h} $(C_4H_4)_2Ni$ (**5**). In the complexes **3** and **4**, one Ni atom is sandwiched by two **1** and **2** ligands, respectively, from the opposite ends along the twofold axis, forming the staggered D_{2d} complexes with Ni-B distances of r_{Ni-B} = 2.10 and 2.11 Å, respectively. These complexes follow the 18-electron rule for the sandwich complexes. Note that, either in **3** or **4**, the B atom faces an O or S atom from the adjacent ligand. Such staggered D_{2d} complexes (**3** and **4**) are the most stable, which can probably better manage the intramolecular Coulomb repulsion in the systems. The calculated Wiberg bond indices for the Ni center in **3** and **4** are 1.59 and 1.98, respectively, suggesting substantial bonding interactions between the Ni center and the ligands (Table 1). The D_{2d} configuration in **3** and **4** is different from that of D_{4h} $(C_4H_4)_2Ni$ (**5**), but similar to those of $(B_6O_6)_2Cr$ and $(B_6O_6)_2V$.[9,10]

It is worth noting that the structural integrity of both $B_2O_2H_2$ (**1**) and $B_2S_2H_2$ (**2**) are well preserved in the sandwich D_{2d} complexes **3** and **4**. For instance, the B-O and B-S distances in **3** and **4** are 1.43 and 1.86 Å, respectively, which are well comparable to 1.40 Å in **1** and 1.83 Å in **2**. Similarly, the natural atomic charges and Wiberg bond indices retained largely unchanged in the **3** and **4** complexes with respect to those in the **1** and **2** ligands, respectively (Table 1). It is interesting to note that the slightly distorted $B_2S_2H_2$ (**2**) becomes completely planar in the sandwich D_{2d} $(B_2S_2H_2)_2Ni$ (**4**) complex. The calculated VIPs for the sandwich complexes D_{2d} $(B_2O_2H_2)_2Ni$ (**3**) and D_{2d} $(B_2S_2H_2)_2Ni$ (**4**) are 8.26 and 8.46 eV at the B3LYP level, respectively, which are markedly higher than that of D_{4h} $(C_4H_4)_2Ni$ (**5**) (7.28 eV). Thus, D_{2d} $(B_2O_2H_2)_2Ni$ (**3**) and D_{2d} $(B_2S_2H_2)_2Ni$ (**4**) are electronically quite stable.

To further evaluate the thermodynamic stabilities of the sandwich complexes **3** and **4**, their formation energies (FEs) are calculated according to the following equations:

$$Ni(^3D) + 2B_2O_2H_2(1, D_{2h,}{}^1A_g) = (B_2O_2H_2)_2Ni(3, D_{2d,}{}^1A_1)$$

$$Ni(^3D) + 2B_2S_2H_2(2, C_{2v,}{}^1A_1) = (B_2S_2H_2)_2Ni(4, D_{2d,}{}^1A_1)$$

The FEs are evaluated by taking into consideration of the free energy corrections. As shown in Table 1, the FEs are 6.21 and −51.28 kcal/mol, respectively, for D_{2d} $(B_2O_2H_2)_2Ni$ (**3**) and D_{2d} $(B_2S_2H_2)_2Ni$ (**4**), suggesting that the former complex is not stable thermodynamically and additional strategies should be sought in order to stabilize such B_2O_2 complexes. However, the FE for **4** is substantial, which indicates that its formation is highly exothermic and energetically favorable. Similar to the η^4-heterocyclic $(C_2P_2R_2)_2Ni$ sandwich complex,[40,41] the $(B_2S_2H_2)_2Ni$ (**4**) complexe may be viable targets for forthcoming synthetic efforts.

Conclusions

In conclusion, we report on the theoretical prediction of two ternary B-O-H and B-S-H rhombic clusters, D_{2h} $B_2O_2H_2$ (**1**) and C_{2v} $B_2S_2H_2$ (**2**), which are the global-minimum structures based on global searches and electronic structure calculations at the B3LYP and CCSD(T) levels. These clusters feature the heteroatomic B_2X_2 (X = O and S) four-membered rings as the core, with two H attached terminally. Chemical bonding analyses show that the **1** and **2** clusters are 4π systems with a rhombic 4c-4e o-bond, in which the two π orbitals are in a nonbonding/bonding combination, effectively making the species as 2π systems with weak aromaticity. The current result also helps shed light on the bonding nature of the relevant $B_2N_2H_4$ species and suggests that it is not an inorganic analogue of antiaromatic cyclobutadiene. In the four-membered 4π systems, aromaticity follows the order: $B_2S_2H_2$ (**2**) > $B_2N_2H_4$ > $B_2O_2H_2$ (**1**) > C_4H_4 (antiaromatic); that is, the large electronegativity difference between B and X (X = N, O, and S), the weaker aromaticity for the system. To aid their future experimental characterizations, the electronic properties of D_{2h} $B_2O_2H_2$ (**1**) and C_{2v} $B_2S_2H_2$ (**2**) are predicted. Lastly, the sandwich-type D_{2d} $(B_2O_2H_2)_2Ni$ (**3**) and D_{2d} $(B_2S_2H_2)_2Ni$ (**4**) complexes are designed computationally to explore the potential use of D_{2h} $B_2O_2H_2$ (**1**) and C_{2v} $B_2S_2H_2$ (**2**) as ligands. A natural question is whether such sandwich-type complexes can be extended to form one-dimensional transition metal sandwich polymers $[Ni(B_2X_2H_2)]_\infty$ (X = O and S), which are worth pursuing in the forthcoming studies.

Acknowledgements

This work was supported by the National Natural Science Foundation of China (21243004, 21373130), the Natural Science Foundation of Shandong Province (ZR2014BL011), the Major Task of Binzhou University (2014ZDL03), and the State Key Laboratory of Quantum Optics and Quantum Optics Devices (KF201402). H.J.Z. gratefully acknowledges the start-up fund from Shanxi University for support.

References

1 a) I. Boustani, *Phys. Rev. B* **1997**, *55*, 16426; b) J. E. Fowler, J. M. Ugalde, *J. Phys. Chem. A* **2000**, *104*, 397; c) J. Aihara, *J. Phys. Chem. A* **2001**, *105*, 5486; d) J. Aihara, H. Kanno, T. Ishida, *J. Am. Chem. Soc.* **2005**, *127*, 13324.

2 H. J. Zhai, A. N. Alexandrova, K. A. Birch, A. I. Boldyrev, L. S. Wang, *Angew. Chem. Int. Ed*. **2003**, *42*, 6004.

3 H. J. Zhai, B. Kiran, J. Li, L. S. Wang, *Nature Mater*. **2003**, *2*, 827.

4 H. J. Zhai, Y. F. Zhao, W. L. Li, Q. Chen, H. Bai, H. S. Hu, Z. A. Piazza, W. J. Tian, H. G. Lu, Y. B. Wu, Y. W. Mu, G. F. Wei, Z. P. Liu, J. Li, S. D. Li, L. S. Wang, *Nature Chem.* **2014**, *6*, 727.

5 a) A. P. Sergeeva, D. Y. Zubarev, H. J. Zhai, A. I. Boldyrev, L. S. Wang, *J. Am. Chem. Soc.* **2008**, *130*, 7244; b) W. Huang, A. P. Sergeeva, H. J. Zhai, B. B. Averkiev, L. S. Wang, A. I. Boldyrev, *Nature Chem.* **2010**, *2*, 202; c) A. P. Sergeeva, Z. A. Piazza, C. Romanescu, W. L. Li, A. I. Boldyrev, L. S. Wang, *J. Am. Chem. Soc.* **2012**, *134*, 18065; d) Q. Chen, G. F. Wei, W. J. Tian, H. Bai, Z. P. Liu, H. J. Zhai, S. D. Li, *Phys. Chem. Chem. Phys.* **2014**, *16*, 18282; e) W. L. Li, Q. Chen, W. J. Tian, H. Bai, Y. F. Zhao, H. S. Hu, J. Li, H. J. Zhai, S. D. Li, L. S. Wang, *J. Am. Chem. Soc.* **2014**, *136*, 12257.

6 A. N. Alexandrova, A. I. Boldyrev, H. J. Zhai, L. S. Wang, *Coord. Chem. Rev.* **2006**, *250*, 2811.

7 a) D. Z. Li, Q. Chen, Y. B. Wu, H. G. Lu, S. D. Li, *Phys. Chem. Chem. Phys.* **2012**, *14*, 14769; b) H. Bai, Q. Chen, C. Q. Miao, Y. W. Mu, Y. B. Wu, H. G. Lu, H. J. Zhai, S. D. Li, *Phys. Chem. Chem. Phys.* **2013**, *15*, 18872; c) H. J. Zhai, Q. Chen, H. Bai, H. G. Lu, W. L. Li, S. D. Li, L. S. Wang, *J. Chem. Phys.* **2013**, *139*, 174301.

8 a) H. J. Zhai, Q. Chen, H. Bai, S. D. Li, L. S. Wang, *Acc. Chem. Res.* **2014**, *47*, 2435; b) H. J. Zhai, S. D. Li, L. S. Wang, *J. Am. Chem. Soc.* **2007**, *129*, 9254; c) S. D. Li, H. J. Zhai, L. S. Wang, *J. Am. Chem. Soc.* **2008**, *130*, 2573.

9 D. Z. Li, H. Bai, Q. Chen, H. G. Lu, H. J. Zhai, S. D. Li, *J. Chem. Phys.* **2013**, *138*, 244304.

10 D. Z. Li, S. G. Zhang, J. J. Liu, C. Tang, *Eur. J. Inorg. Chem.* **2014**, 3406.

11 D. Z. Li, C. C. Dong, S. G. Zhang, *J. Mol. Model.* **2013**, *19*, 3219.

12 a) Q. Chen, H. Bai, J. C. Guo, C. Q. Miao, S. D. Li, *Phys. Chem. Chem. Phys.* **2011**, *13*, 20620; b) D. Z. Li, H. G. Lu, S. D. Li, *J. Mol. Model.* **2012**, *18*, 3161; c) Q. Chen, S. D. Li, *J. Clust. Sci.* **2011**, *22*, 513.

13 D. Z. Li, H. Bai, T. Ou, Q. Chen, H. J. Zhai, S. D. Li, *J. Chem. Phys.* **2015**, *142*, 014302.

14 J. A. Tossell, J. H. Moore, K. Mcmillan, C. K. Cubramaniam, M. A. Coplan, *J. Am. Chem. Soc.* **1992**, *114*, 1114.

15 L. Barton, F. A. Grimm, R. F. Porter, *Inorg. Chem.* **1966**, *5*, 2076.

16 W. Harshbarger, G. H. Lee II, R. F. Forter, S. H. Bauer, *Inorg. Chem.* **1969**, *8*, 1683.

17 P. W. Fowler, E. Steiner, *J. Phys. Chem. A* **1997**, *101*, 1409.

18 J. J. Engelberts, R. W. A. Havenith, J. H. van Lenthe, L. W. Jenneskens, P. W. Fowler, *Inorg. Chem.* **2005**, *44*, 5266.

19 C. H. Chang, R. F. Porter, S. H. Bauer, *Inorg. Chem.* **1969**, *8*, 1689.

20 J. A. Tossell, P. Lazzeretti, *J. Phys. Chem.* **1990**, *94*, 1723.

21 K. L. Bhat, G. D. Markham, J. D. Larkin, C. W. Bock, *J. Phys. Chem. A* **2011**, *115*, 7785.

22 a) N. C. Baird, R. K. Datta, *Inorg. Chem.* **1972**, *11*, 17; b) N. C. Baird, *Inorg. Chem.* **1973**, *12*, 473.

23 A. J. Bridgeman, J. Rothery, *Inorg. Chim. Acta* **1999**, *288*, 17.

24 A. Rehaman, A. Datta, S. S. Mallajosyula, S. K. Pati, *J. Chem. Theory Comput.* **2006**, *2*, 30.

25 Q. Chen, H. G. Lu, H. J. Zhai, S. D. Li, *Phys. Chem. Chem. Phys.* **2014**, *16*, 7274.

26 a) D. Y. Zubarev, A. I. Boldyrev, *Phys. Chem. Chem. Phys*. **2008**, *10*, 5207; b) D. Y. Zubarev, A. I. Boldyrev, *J. Org. Chem*. **2008**, *73*, 9251; c) D. Y. Zubarev, A. I. Boldyrev, *J. Phys. Chem. A* **2009**, *113*, 866; d) T. R. Galeev, Q. Chen, J. C. Guo, H. Bai, C. Q. Miao, H. G. Lu, A. P. Sergeeva, S. D. Li, A. I. Boldyrev, *Phys. Chem. Chem. Phys*. **2011**, *13*, 11575.

27 A. N. Alexandrova, A. I. Boldyrev, Y. J. Fu, X. Yang, X. B. Wang, L. S. Wang, *J. Chem. Phys*. **2004**, *121*, 5709.

28 A. N. Alexandrova, A. I. Boldyrev, *J. Chem. Theory Comput*. **2005**, *1*, 566.

29 A. P. Sergeeva, B. B. Averkiev, H. J. Zhai, A. I. Boldyrev, L. S. Wang, *J. Chem. Phys*. **2011**, *134*, 224304.

30 a) M. Saunders, *J. Comput. Chem*. **2004**, *25*, 621; b) P. P. Bera, K. W. Sattelmeyer, M. Saunders, H. F. Schaefer III, P. v. R. Schleyer, *J. Phys. Chem. A* **2006**, *110*, 4287.

31 A. D. Becke, *J. Chem. Phys*. **1993**, *98*, 5648.

32 C. Lee, W. Yang, R. G. Parr, *Phys. Rev. B* **1988**, *37*, 785.

33 M. J. Frisch, G. W. Trucks, H. B. Schlegel, G. E. Scuseria, *et al*., GAUSSIAN 03, Revision A.01, Gaussian, Inc., Wallingford, CT, 2004.

34 Stuttgart RSC 1997 ECP basis sets used in this work and the related references therein can be obtained from https://bse.pnl.gov/bse/portal.

35 J. Cizek, *Adv. Chem. Phys*. **1969**, *14*, 35.

36 a) G. E. Scuseria, H. F. Schaefer III, *J. Chem. Phys*. **1989**, *90*, 3700; b) G. E. Scuseria, C. L. Janssen, H. F. Schaefer III, *J. Chem. Phys*. **1988**, *89*, 7382.

37 J. A. Pople, M. Head-Gordon, K. Raghavachari, *J. Chem. Phys*. **1987**, *87*, 5968.

38 E. D. Glendening, J. K. Badenhoop, A. E. Reed, J. E. Carpenter, J. A. Bohmann, C. M. Morales, F. Weinhold, NBO 5.0, Theoretical Chemistry Institute, University of Wisconsin, Madison, WI, 2001.

39 W. Kutzelnigg, *Angew. Chem. Int. Ed. Engl*. **1984**, *23*, 272.

40 M. D. Su, S.Y. Chu, *J. Phys. Chem.* **1991**, *95*, 9757.

41 T. Wettling, G. Wolmershauser, P. Binger, M. Regitz, *J. Chem. Soc. Chem. Commun*. **1990**, *21*, 1541.

Table 1. Natural atomic charges of the B_2X_2 rings (q; in |e|), lowest vibrational frequencies (ν_{min}, in cm^{-1}), Wiberg bond indices (WBIs) of D_{2h} $B_2O_2H_2$ (**1**), C_{2v} $B_2S_2H_2$ (**2**), and their relevant sandwich-type complexes (**3–5**). The vertical ionization potentials (VIPs, in eV) and the formation energies (FEs, in kcal/mol) are also listed. Free energy corrections are included in the FEs.

	q_B	q_X	ν_{min}	WBI_B	WBI_X	WBI_M	VIP	FE
D_{2h} $B_2O_2H_2$ (**1**)	0.95	−0.86	226.4	2.81	1.84	-	12.25	-
C_{2v} $B_2S_2H_2$ (**2**)	0.16	−0.11	163.6	3.50	2.53	-	9.55	-
D_{2d} $(B_2O_2H_2)_2Ni$ (**3**)	0.77	−0.79	85.8	3.05	1.90	1.59	8.26	6.21
D_{2d} $(B_2S_2H_2)_2Ni$ (**4**)	0.08	0.05	68.1	3.67	2.64	1.98	8.46	−51.28
D_{4h} $(C_4H_4)_2Ni$ (**5**)	-	-	48.9	-	-	2.17	7.28	−102.8

Figure Captions

Fig. 1 Global-minimum structures of D_{2h} $B_2O_2H_2$ (**1**, ^1A_g) and C_{2v} $B_2S_2H_2$ (**2**, $^1A_1$) at the B3LYP/aug-cc-pVTZ level. Selected bond distances are labeled in angstroms. Both the top view and side view (dihedral angle shown in degrees) are presented for **2**. The B atom is in pink, O in red, S in yellow, and H in gray.

Fig. 2 Alternative optimized low-lying structures of $B_2O_2H_2$. Relative energies are indicated in eV at the B3LYP/aug-cc-pVTZ level with zero-point energy (ZPE) corrections, as well as at the CCSD(T)//B3LYP/aug-cc-pVTZ level (in the parentheses). The B, O, and H atoms are in pink, red, and gray, respectively.

Fig. 3 The AdNDP bonding pattern of D_{2h} $B_2O_2H_2$ (**1**, ^1A_g). Occupation numbers (ONs) are shown.

Fig. 4 Comparison of the π bonding systems of $B_2O_2H_2$ (D_{2h}, ^1A_g), $B_2S_2H_2$ (C_{2v}, $^1A_1$), and cyclobutadiene.

Fig. 5 Alternative optimized low-lying structures of $B_2S_2H_2$. Note that the D_{2h} (^1A_g) structure is a transition state. Relative energies are indicated in eV at the B3LYP/aug-cc-pVTZ level with zero-point energy (ZPE) corrections, as well as at the CCSD(T)//B3LYP/aug-cc-pVTZ level (in the parentheses). The B, S, and H atoms are in pink, yellow, and gray, respectively.

Fig. 6 The AdNDP bonding pattern of C_{2v} $B_2S_2H_2$ (**2**, $^1A_1$). Occupation numbers (ONs) are shown.

Fig. 7 Simulated infrared (IR) spectrum of $B_2O_2H_2$ (D_{2h}, ^1A_g) and $B_2S_2H_2$ (C_{2v}, $^1A_1$).

Fig. 8 Sandwich-type complexes D_{2d} $(B_2O_2H_2)_2Ni$ (**3**) and D_{2d} $(B_2S_2H_2)_2Ni$ (**4**) at the B3LYP level, as compared with their cyclobutadiene counterpart, D_{4h} $(C_4H_4)_2Ni$ (**5**). Selected bond distances are labeled in angstroms. The B atom is in pink, O in red, S in yellow, and C and H in gray.

Fig. 1

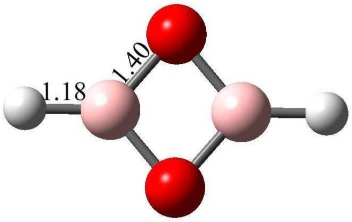

1 D_{2h} $B_2O_2H_2$ (^1A_g)

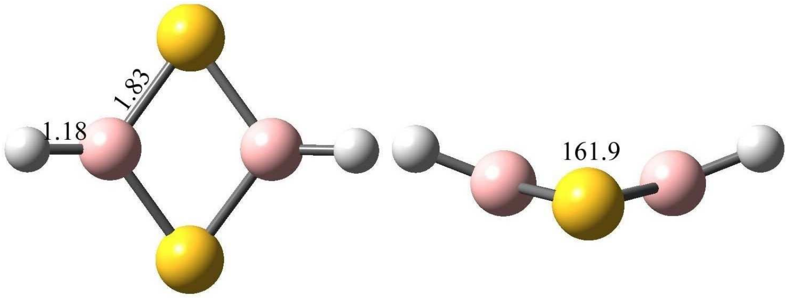

2 C_{2v} $B_2S_2H_2$ ($^1A_1$)

Fig. 2

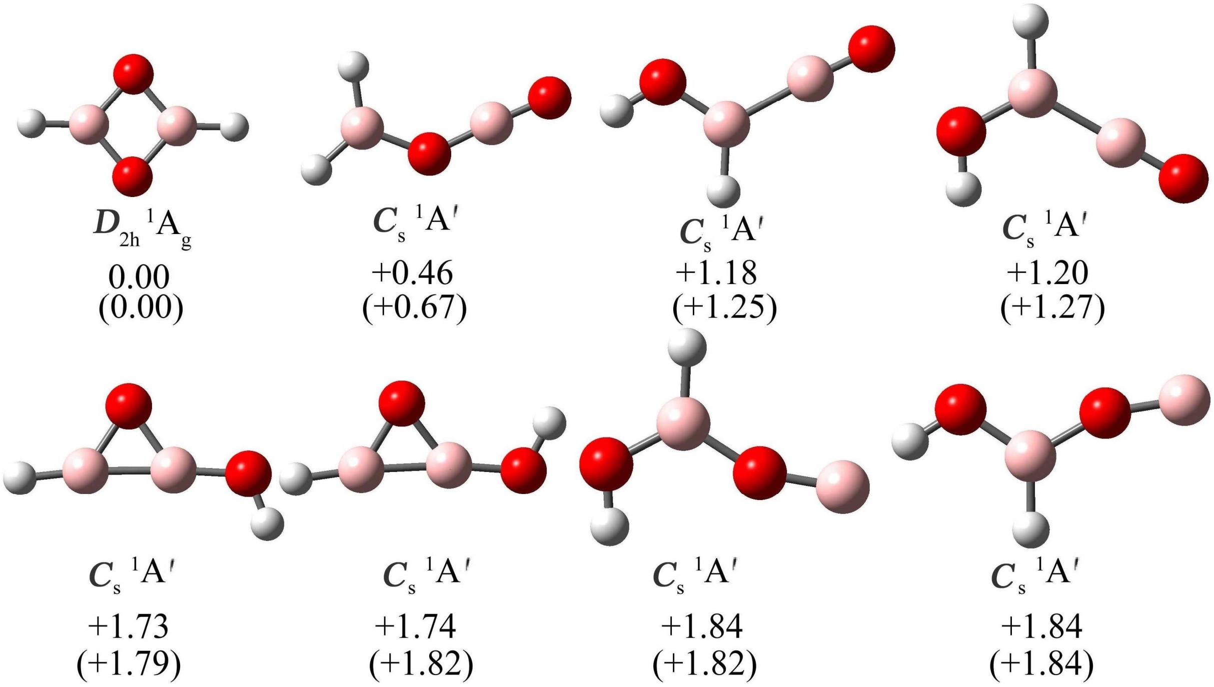
D_{2h} ^1A_g
0.00
(0.00)
C_s $^1A'$
+0.46
(+0.67)
C_s $^1A'$
+1.18
(+1.25)
C_s $^1A'$
+1.20
(+1.27)
C_s $^1A'$
+1.73
(+1.79)
C_s $^1A'$
+1.74
(+1.82)
C_s $^1A'$
+1.84
(+1.82)
C_s $^1A'$
+1.84
(+1.84)

Fig. 3

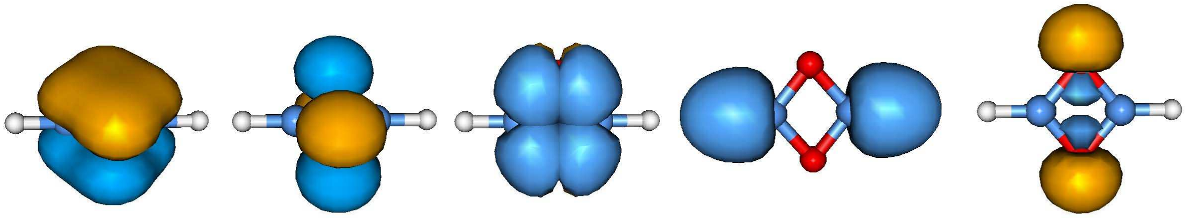

1×4c-2e π ON=2.00 |e|

1×2c-2e O-O π ON=2.00 |e|

4×2c-2e B-O σ ON=1.98 |e|

2×2c-2e B-H σ ON=1.99 |e|

2×1c-2e O lone pairs ON=1.97 |e|

Fig. 4

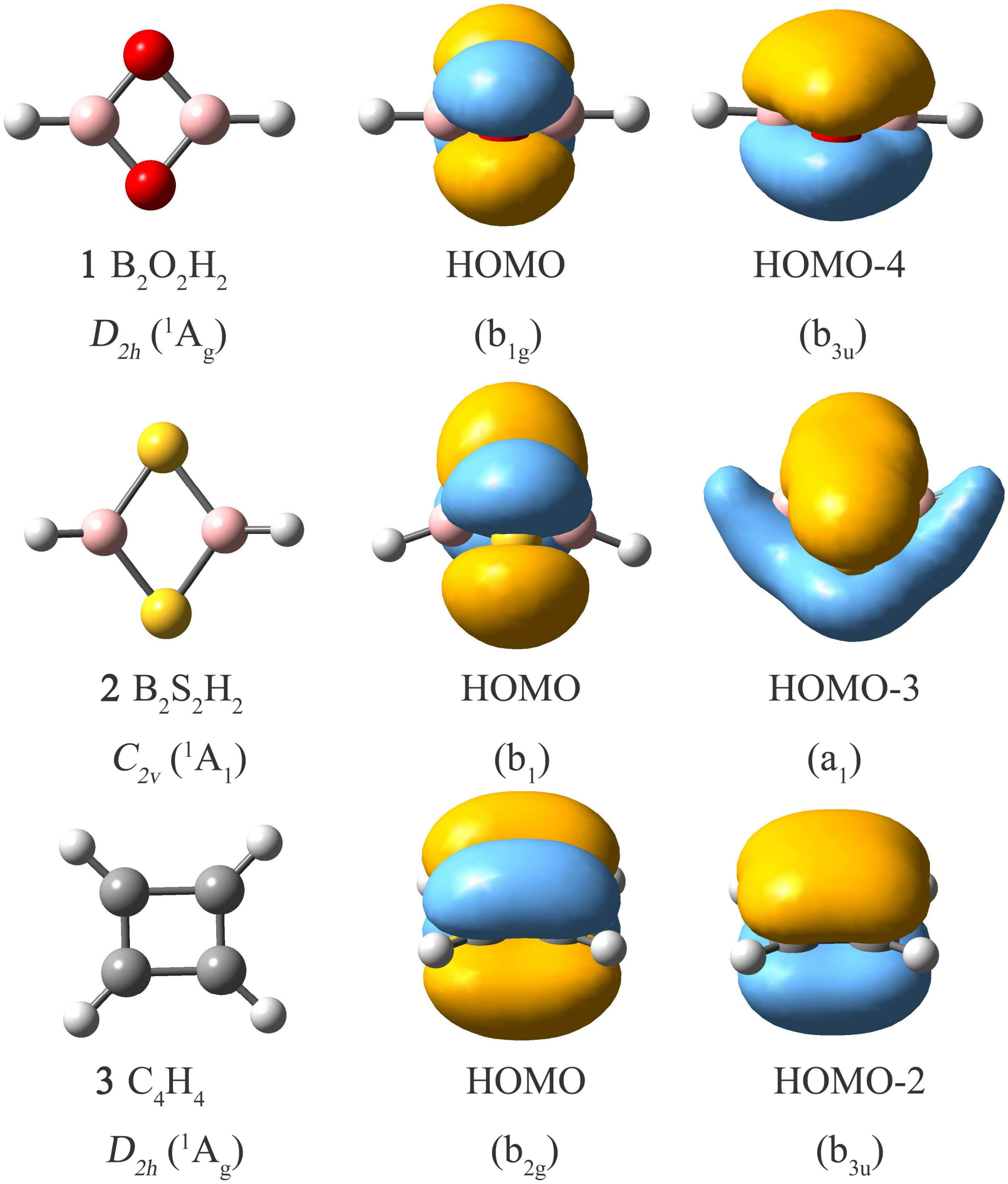
1 $B_2O_2H_2$
D_{2h} (^1A_g)
HOMO
(b_{1g})
HOMO-4
(b_{3u})
2 $B_2S_2H_2$
C_{2v} ($^1A_1$)
HOMO
(b_1)
HOMO-3
(a_1)
3 C_4H_4
D_{2h} (^1A_g)
HOMO
(b_{2g})
HOMO-2
(b_{3u})

Fig. 5

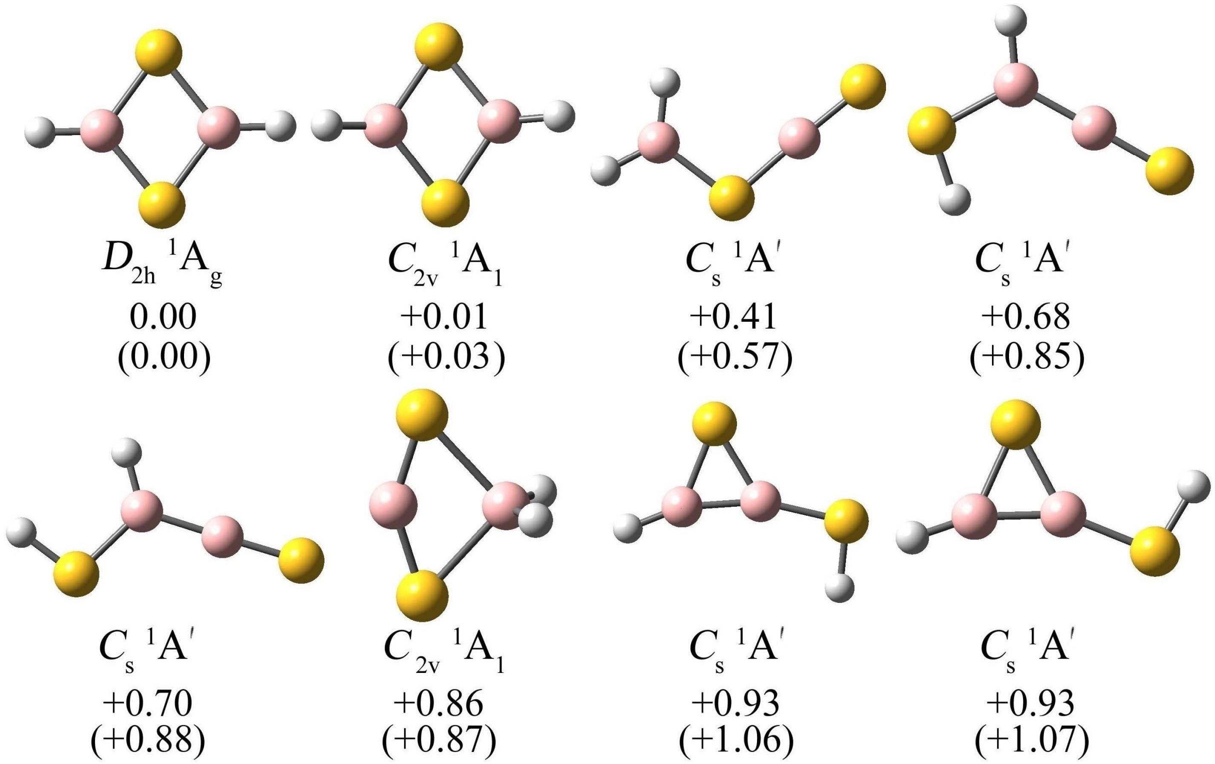
D_{2h} ^1A_g
0.00
(0.00)
C_{2v} $^1A_1$
+0.01
(+0.03)
C_s $^1A'$
+0.41
(+0.57)
C_s $^1A'$
+0.68
(+0.85)
C_s $^1A'$
+0.70
(+0.88)
C_{2v} $^1A_1$
+0.86
(+0.87)
C_s $^1A'$
+0.93
(+1.06)
C_s $^1A'$
+0.93
(+1.07)

Fig. 6

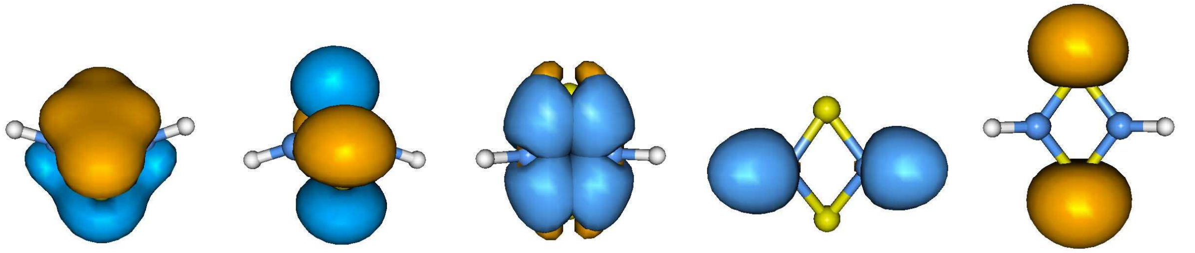

1×4c-2e π ON=2.00 |e|

1×2c-2e S-S π ON=2.00 |e|

4×2c-2e B-S σ ON=1.96 |e|

2×2c-2e B-H σ ON=1.97 |e|

2×1c-2e S lone pairs ON=2.00 |e|

Fig. 7

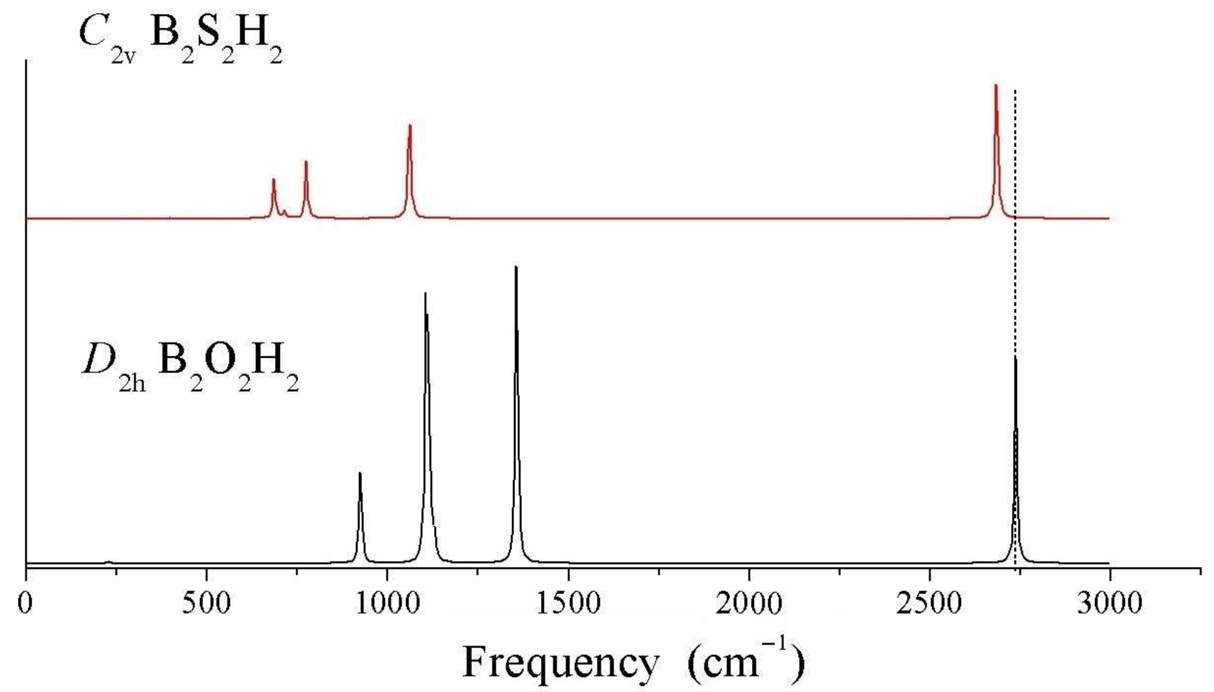
C_{2v} $B_2S_2H_2$
D_{2h} $B_2O_2H_2$
0
500
1000
1500
2000
2500
3000
Frequency (cm^{-1})

Fig. 8

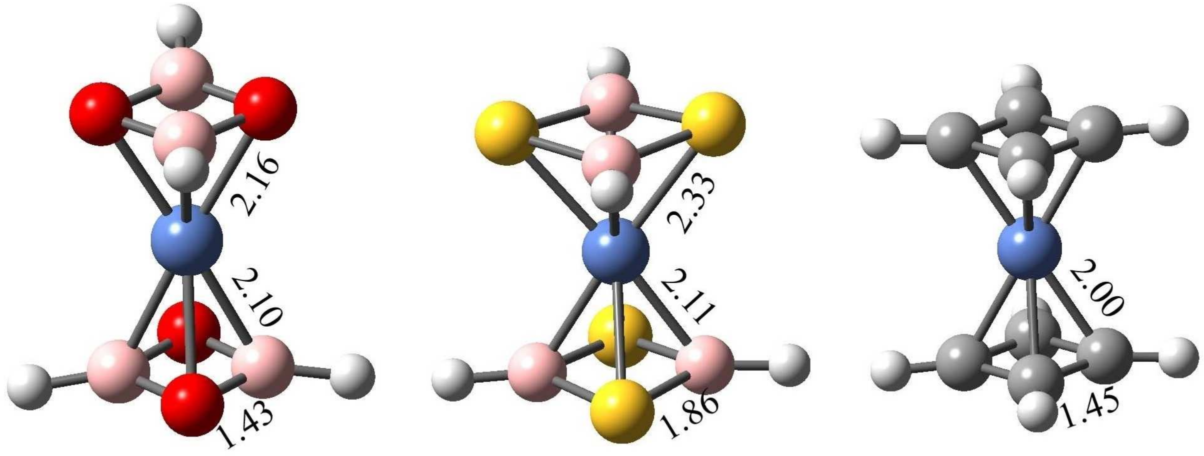

3 D_{2d} $(B_2O_2H_2)_2Ni$ ($^1A_1$) **4** D_{2d} $(B_2S_2H_2)_2Ni$ ($^1A_1$) **5** D_{4h} $(C_4H_4)_2Ni$ ($^1A_{1g}$)